Article

Cell Reports

# Notch2 Is Required for Inflammatory Cytokine-Driven Goblet Cell Metaplasia in the Lung

## Graphical Abstract

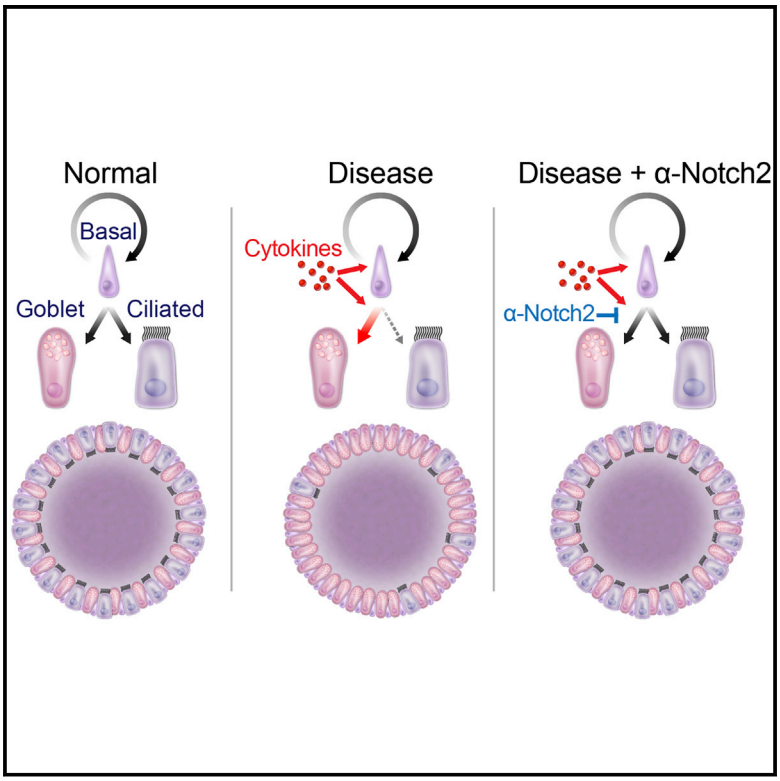


## Authors

Henry Danahay, Angelica D. Pessotti, ..., Marc Hild, Aron B. Jaffe

## Correspondence

h.danahay@sussex.ac.uk (H.D.), aron.jaffe@novartis.com (A.B.J.)

## In Brief

Goblet cell metaplasia, resulting in excessive mucus production, is a hallmark of airway diseases. Here, Danahay et al. demonstrate that inhibition of Notch2 prevents goblet cell metaplasia in response to diverse stimuli in vitro and in vivo, validating Notch2 blockade as a therapeutic strategy for airway diseases.

## Highlights

- Airway basal cells differentiate into goblet and ciliated cells in 3D cultures
- Inflammatory cytokines bias airway basal cell fate to drive goblet cell metaplasia
- Notch2 is a key node required for goblet cell metaplasia
- Targeting Notch2 prevents goblet cell metaplasia, regardless of the stimulus

Danahay et al., 2015, Cell Reports *10*, 239–252
January 13, 2015 
http://dx.doi.org/10.1016/j.celrep.2014.12.017

CellPress

Cell Reports
Article



# Notch2 Is Required for Inflammatory Cytokine-Driven Goblet Cell Metaplasia in the Lung

Henry Danahay,[1,5,*] Angelica D. Pessotti,[2] Julie Coote,[1] Brooke E. Montgomery,[2] Donghui Xia,[2] Aaron Wilson,[2] Haidi Yang,[2] Zhao Wang,[2] Luke Bevan,[1] Chris Thomas,[2] Stephanie Petit,[2] Anne London,[3] Peter LeMotte,[3] Arno Doelemeyer,[4] Germán L. Vélez-Reyes,[2] Paula Bernasconi,[2] Christy J. Fryer,[2] Matt Edwards,[1] Paola Capodieci,[2] Amy Chen,[2] Marc Hild,[2] and Aron B. Jaffe[2,*]

[1]Respiratory Disease Area, Novartis Institutes for BioMedical Research, Horsham RH12 5AB, UK
[2]Developmental and Molecular Pathways
[3]Novartis Biologics Center
Novartis Institutes for BioMedical Research, 250 Massachusetts Avenue, Cambridge, MA 02139, USA
[4]Discovery and Investigative Pathology, Novartis Institutes for BioMedical Research, 4002 Basel, Switzerland
[5]Present address: School of Life Sciences, University of Sussex, Brighton BN1 9RH, UK
*Correspondence: h.danahay@sussex.ac.uk (H.D.), aron.jaffe@novartis.com (A.B.J.)
http://dx.doi.org/10.1016/j.celrep.2014.12.017


## SUMMARY

**The balance and distribution of epithelial cell types is required to maintain tissue homeostasis. A hallmark of airway diseases is epithelial remodeling, leading to increased goblet cell numbers and an overproduction of mucus. In the conducting airway, basal cells act as progenitors for both secretory and ciliated cells. To identify mechanisms regulating basal cell fate, we developed a screenable 3D culture system of airway epithelial morphogenesis. We performed a high-throughput screen using a collection of secreted proteins and identified inflammatory cytokines that specifically biased basal cell differentiation toward a goblet cell fate, culminating in enhanced mucus production. We also demonstrate a specific requirement for Notch2 in cytokine-induced goblet cell metaplasia in vitro and in vivo. We conclude that inhibition of Notch2 prevents goblet cell metaplasia induced by a broad range of stimuli and propose Notch2 neutralization as a therapeutic strategy for preventing goblet cell metaplasia in airway diseases.**

## INTRODUCTION

The lung epithelium has evolved to serve a number of functions, ranging from gas exchange in the alveolus to the regulation of mucus clearance in the larger conducting airways. The heterogeneous mix of epithelial cell types enables these functions at the different levels of the airway. For example, mucin-producing and secreting goblet cells provide a mucus gel that the multiciliated cells propel in a cephalad direction out of the airways, whereas surfactant-producing type 2 pneumocytes maintain alveolar patency with type 1 pneumocytes enabling gas exchange (Rackley and Stripp, 2012). A greater understanding of the pathways that regulate the function of the epithelium as well as those which define repair and remodeling in both health and disease will be integral to our identification of therapeutic targets to treat respiratory diseases such as severe asthma, cystic fibrosis, and chronic obstructive pulmonary disease (COPD).

A key feature common to many airway diseases is epithelial remodeling, leading to an increase in the number of goblet cells and an overproduction of mucus, called "goblet cell metaplasia" (gcm) (Fahy and Dickey, 2010). An inability to clear the increased mucus can lead to airflow obstruction, mucostasis, and ultimately death (Hogg et al., 2004; Kuyper et al., 2003; Lange et al., 1998). Whereas an increase in several cytokines and growth factors has been associated with airway diseases such as asthma (Finkelman et al., 2010), only interleukin (IL)-13, and the closely related cytokine IL-4, acting through a shared receptor, have been shown to directly affect the airway epithelium to increase goblet cell formation (Atherton et al., 2003; Dabbagh et al., 1999; Grünig et al., 1998; Kuperman et al., 2002; Laoukili et al., 2001; Munitz et al., 2008). IL-13 is a key marker of the "Th2-high" asthma phenotype, which is seen in approximately 50% of patients with asthma (Woodruff et al., 2009). A recent clinical trial with anti-IL-13 antibodies has demonstrated improved airflow in patients with asthma, and this improvement was more pronounced in patients with increased levels of periostin, a downstream target of IL-13 (Corren et al., 2011). The factors that drive gcm in asthmatics with a "Th2-low" phenotype, as well as patients with COPD and cystic fibrosis (CF), are less well defined.

In the present study, we describe the analysis of a method for the 3D culture of primary human airway basal cells (bronchospheres). Developing bronchospheres respond to IL-13 with an increase in the expression of markers of goblet cells and a decline in ciliated cell number. We conducted a high-throughput screen for secreted factors that influence bronchosphere development and found a number of proteins that can bias basal cell differentiation toward a goblet cell fate, thereby altering the composition of the airway epithelium to produce the goblet cell

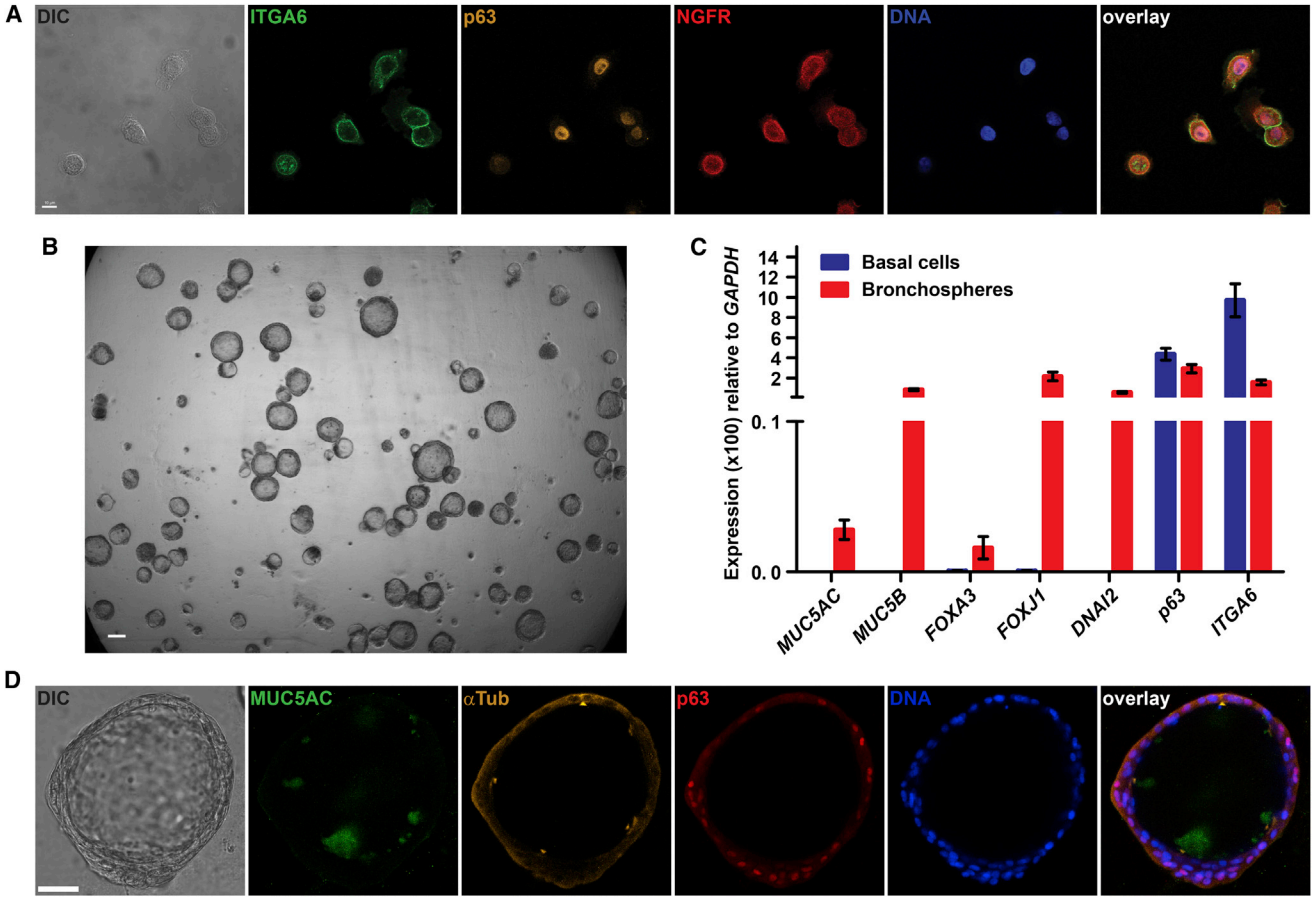


**Figure 1. Human Airway Basal Cells Form "Bronchospheres" in 3D Culture**

(A) Human airway basal cells were grown overnight in chambered slides and stained for integrin α6 (ITGA6, green), p63 (orange), nerve growth factor receptor (NGFR) (red), and DNA (blue). Note that all of the cells are positive for the airway basal cell markers ITGA6, p63, and NGFR. The DIC image is shown on the left, and the overlay is on the right. The scale bar represents 10 μm.

(B) Phase contrast image of day 14 bronchospheres. The scale bar represents 100 μm.

(C) Quantitative PCR analysis of goblet (*MUC5AC*, *MUC5B*, and *FOXA3*), ciliated (*FOXJ1* and *DNAI2*), and basal cell markers (*p63* and *ITGA6*) expressed by airway basal cells grown on plastic or after 14 days of growth in 3D into bronchospheres. Shown is the average ± SEM of at least four independent donors.

(D) Day 14 bronchospheres were fixed and stained for DNA (blue) and markers of basal cells (p63, red), ciliated cells (acetylated α-tubulin, orange), and goblet cells (MUC5AC, green). The scale bar represents 50 μm.

metaplasia described in many respiratory diseases. Finally, we demonstrate that Notch2 is absolutely required for goblet cell metaplasia in vitro and in vivo. We propose that Notch2 represents a novel therapeutic target for the prevention of goblet cell metaplasia in human respiratory diseases such as asthma, COPD, and CF.

## RESULTS

### Human Airway Basal Cells Form "Bronchospheres" in 3D Culture

Prior to plating primary human airway basal cells in Matrigel in 3D, we confirmed that they expressed the basal cell markers p63, nerve growth factor receptor (NGFR), and ITGA6 (Figure 1A). Immediately after seeding $p63^+NGFR^+ITGA6^+$ basal cells in Matrigel, the cells aggregated to form balls of cells that continued to proliferate (Movie S1). Lumen formation initiated between days 8 and 10 in 3D (Movie S2; Figure S1D), and by day 14, the majority of structures contained a central lumen (Figure 1B). Immunostaining revealed $p63^+$ cells basal to the cells lining the interior of the cyst, consistent with a pseudostratified structure. In contrast, cells lining the central lumen were invariably negative for Ki67 staining (data not shown). Ciliated cells, detected by acetylated α-tubulin staining, were identified lining the central lumen (Figure 1D). Furthermore, prior to fixation, the rapid beating of these cilia could be observed under bright-field conditions (Movies S3 and S4). In addition to ciliated cells, $MUC5AC^+$ goblet cells were also identified lining the central lumen (Figure 1D). $MUC5AC^+$ material was also seen inside of the central lumen consistent with secretion of mucins by the epithelium in addition to their storage (Figure 1D). A comparison of the expression of cell-specific markers by quantitative PCR (qPCR) further highlighted the differentiation of the basal cells into a mucociliary epithelium, with the appearance of markers of ciliated (*FOXJ1*

and *DNAI2*) and goblet cells (*MUC5AC*, *MUC5B*, and *FOXA3*; Figures 1C and S1A–S1C).

With the knowledge that bronchospheres were composed of at least three cell types, basal, ciliated, and goblet, we asked whether this heterogeneity was a consequence of mixed populations of precommitted basal cells forming a bronchosphere or whether the basal cells were indeed multipotent, as has been described in the murine trachea (Rock et al., 2009). A clonal seeding threshold was established to be $\leq$75 cells/well of a 384-well plate using a labeled cell-mixing approach (Figure S1E). At this seeding density, bronchospheres formed with an approximately 40% clonal efficiency. Bronchospheres were observed to be composed of basal, goblet, and ciliated cells, confirming the multipotent nature of $p63^+NGFR^+ITGA6^+$ basal cells (Figure S1F). This provides an example of a 3D system that contains the human conducting airway progenitor, the airway basal cell, as well as the two major differentiated cell types that it generates, goblet and ciliated cells, recapitulating the cellular complexity of the conducting airway.

## IL-13 Induces a Mucus Hypersecretory Phenotype in Bronchospheres

We next asked whether bronchospheres could respond to established inducers of airway epithelial remodeling. IL-13 has been shown to be a key mediator of asthmatic phenotypes (Wills-Karp, 2004), and several groups have demonstrated that IL-13 acts directly on the epithelium to drive a goblet cell metaplasia phenotype (Atherton et al., 2003; Kuperman et al., 2002; Laoukili et al., 2001). Treatment of developing bronchospheres with IL-13, between days 2 and 14 after seeding, resulted in an increase in the expression of markers of goblet cells, whereas ciliated cell marker expression declined (Figure S2A). The induction of the remodeled phenotype was concentration dependent, with the highest concentrations impairing differentiation, consistent with previous observations using air-liquid interface (ALI) human bronchial epithelial (HBE) cultures (Atherton et al., 2003). The enhanced expression of goblet cell markers was difficult to observe and quantify by immunofluorescence in bronchospheres, largely due to the accumulation of secreted mucins in the central lumen during culture. However, the loss of ciliated cell marker expression was confirmed by a lack of acetylated $\alpha$-tubulin-positive structures in the IL-13-treated bronchospheres (Figures S2B and S2C).

## Inflammatory Cytokines Alter Basal Cell Fates

Several inflammatory cytokines and growth factors have been reported to increase the expression of MUC5AC in airway epithelial cells (Chen et al., 2003; Fujisawa et al., 2009; Gray et al., 2004; Kim et al., 2002). However, only IL-13, and the closely related cytokine IL-4, acting through a shared receptor, have been shown to act directly on the epithelium to drive a goblet cell metaplasia phenotype, resulting in increased numbers of goblet cells and fewer ciliated cells (Atherton et al., 2003; Dabbagh et al., 1999; Grünig et al., 1998; Kuperman et al., 2002; Laoukili et al., 2001; Munitz et al., 2008). Goblet cell metaplasia is a hallmark of several airway diseases, including asthma and COPD (Fahy and Dickey, 2010), and whether soluble factors other than IL-13 act directly on the epithelium to drive this phenotype is not known. To identify novel factors that regulate airway basal cell fate leading to a goblet cell metaplasia phenotype, we screened a collection of 4,876 secreted, recombinant human proteins, representing 2,366 unique gene products (Gonzalez et al., 2010) in the bronchosphere assay using cell-type-specific expression markers as endpoints (Figure 2A). Approximately 9% of the recombinant proteins (420/4,876), representing 328 unique gene products, modulated expression of one or more of the cell-type-specific markers by 2-fold or greater (Table S1). The 420 recombinant proteins that affected the assay could be classified into three groups: (1) one or more cell-type-specific markers decreased by 2-fold or greater without a concomitant increase in another marker (323/420); (2) one or more markers of a particular cell type increased by 2-fold or greater without a concomitant decrease of another marker (27/420); and (3) one or more markers of one cell type increased by 2-fold or greater with a concomitant decrease in markers of one or two cell types (70/420; Table S1; Figure 2B).

The effect of the third group of proteins could be further divided into two types of alterations in basal-cell-fate decision. The first was treatments that resulted in an increase in a basal cell marker and a decrease in one or more markers of ciliated cells and/or goblet cells, consistent with inhibition of differentiation. Interestingly, these proteins were almost exclusively members of the epidermal growth factor (EGF) family of ligands (14/15; Figure 2B). The second type of effect was an increase in one or more of the goblet cell markers and a decrease in one or more ciliated or basal cell markers. More than half of these proteins were inflammatory cytokines (33/54), suggesting that, similar to IL-13, many inflammatory cytokines can bias the differentiation of basal cells away from a ciliated cell fate and toward a goblet cell.

## IL-17A Treatment Biases Basal Cell Differentiation toward a Goblet Cell

IL-17A is a cytokine that is secreted by Th17 cells and has been proposed to play a role in severe asthma (Chesné et al., 2014). IL-17A has been shown to stimulate mucin gene expression in cultured airway epithelial cells (Chen et al., 2003) and enhance airway smooth muscle contraction in vivo (Kudo et al., 2012). Whether IL-17A can act directly on airway epithelial cells to alter the composition of the epithelium and result in goblet cell metaplasia is not known. The results from our screen (Figure 2B) and subsequent validation using a broader range of IL-17A concentrations (Figures 3A–3C) indicated that, in addition to increasing *MUC5AC* levels, IL-17A treatment resulted in increased levels of multiple markers of goblet cells (*MUC5B* and *FOXA3*), while inhibiting the expression of markers of ciliated cells (*FOXJ1* and *DNAI2*). These results suggest that IL-17A treatment can bias the differentiation of the airway basal cell toward a goblet cell at the expense of a ciliated cell, a phenotype similar to the goblet cell metaplasia seen in many airway diseases.

To test this hypothesis, we utilized ALI cultures, seeding airway basal cells onto transwell filters, treating the cultures with IL-17A from day 7 (day 0 at ALI), prior to the initiation of differentiation, and analyzing the resulting phenotype at day 21 (day 14 at ALI). Whereas cultures grown under control conditions contained a mixture of goblet and ciliated cells at day 21,

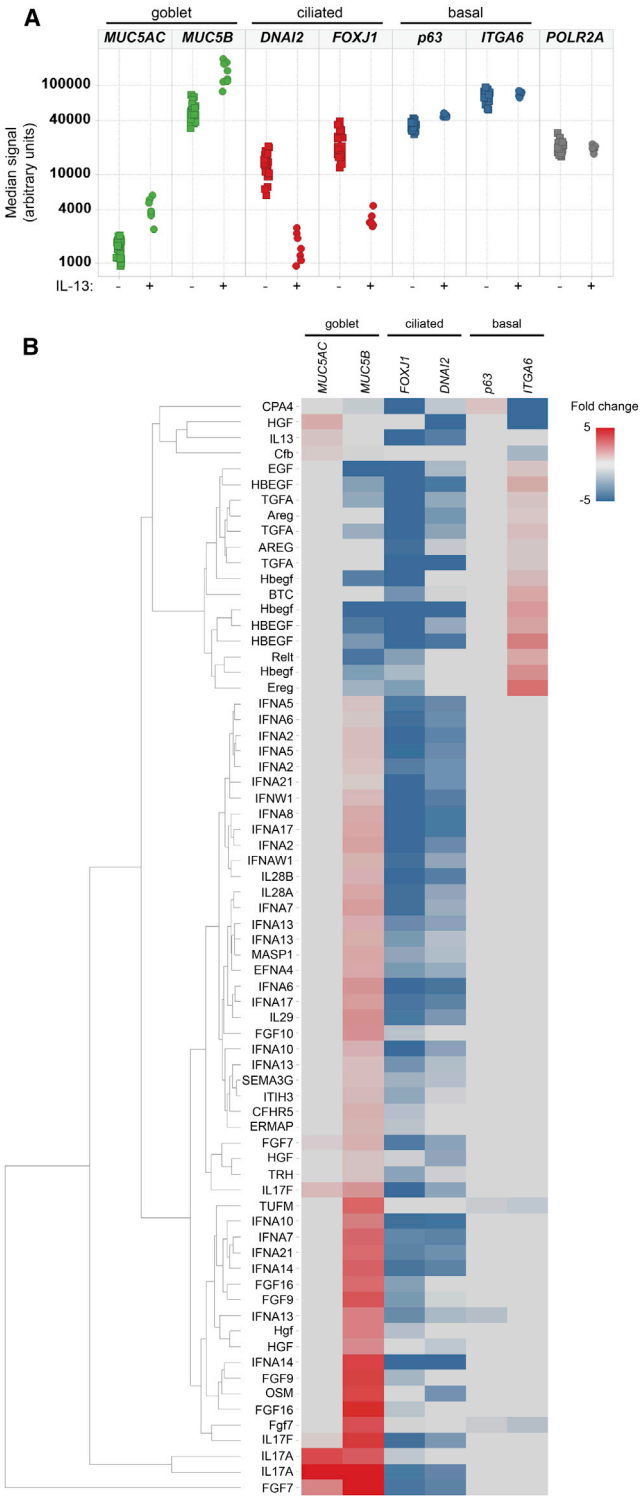


**Figure 2. A Screen of the Mammalian "Secretome" Identifies Multiple Mediators of Goblet Cell Metaplasia In Vitro**

(A) Molecular signature assay to monitor the relative abundance of goblet, ciliated, and basal cells in vitro. Each data point is the median signal from an individual well of a 384-well plate. Note that IL-13 treatment results in an increase in the expression of goblet cell markers and a decrease in the expression of ciliated cell markers, without affecting basal cell markers.

IL-17A-treated cultures had a profound expansion of the goblet cell population, together with a dramatic reduction in the number of ciliated cells (Figures 3D and 3E). Together, our data indicate that IL-17A is sufficient to bias basal cell fate toward a goblet cell and away from a ciliated cell, resulting in a phenotype that is similar to the goblet cell metaplasia seen in many airway diseases.

## Notch2 Is Required for Cytokine-Driven Effects on Basal Cell Fate Specification In Vitro

The Notch-signaling pathway plays a key role in the determination of cell fate in multiple tissues throughout development (Fortini, 2009). To determine the role of Notch in human airway basal cell fate, we first analyzed the expression of Notch receptors in (1) basal cells prior to plating in Matrigel, (2) fully formed (day 14) bronchospheres, and (3) fluorescence-activated-cell-sorting-purified ITGA6$^+$ basal and ITGA6$^-$ luminal cells from day 21 ALI cultures (Figure S3). qPCR analysis of genes that are specifically expressed in basal cells (*p63* and *ITGA6*), goblet cells (*MUC5AC*, *MUC5B*, and *FOXA3*), and ciliated cells (*FOXJ1* and *DNAI2*) confirmed that the ITGA6$^+$ and ITGA6$^-$ populations were enriched for basal cells and differentiated cells, respectively (Figure S3). We found that airway basal cells, either prior to plating in Matrigel or purified from day 21 ALI cultures as well as bronchospheres and luminal cells from day 21 ALI cultures, express *Notch1*, *Notch2*, and *Notch3*, but not *Notch4* (Figure S3). To determine which of the Notch receptors is required for human airway goblet cell formation, we treated developing 3D bronchosphere cultures with Notch1-, Notch2-, or Notch3-receptor-specific blocking antibodies (Li et al., 2008; Wu et al., 2010). We first verified the selectivity of each antibody using Notch-receptor-specific reporter gene assays (Figure S4) and that each antibody inhibited the expression of one or more endogenous Notch target genes in 3D bronchospheres (Bray and Bernard, 2010; Figure S4). All three antibodies inhibited expression of the Notch target gene *NRARP* (Lamar et al., 2001), whereas anti-Notch2 antibodies also inhibited expression of *HEY1* and *HES5*. Anti-Notch3 antibodies also inhibited *HES5* expression, albeit to a lesser degree than anti-N2.

Each Notch-receptor-specific antibody had a distinct effect on 3D bronchospheres (Figures 4A–4C). Anti-Notch1 treatment led to increased levels of multiple markers of basal cells (*p63* and *ITGA6*), without affecting the expression of goblet or ciliated cell markers. Anti-Notch2 antibodies strongly inhibited the expression of all three goblet cell markers (*MUC5AC*, *MUC5B*, and *FOXA3*), while simultaneously increasing expression of multiple ciliated cell markers (*FOXJ1* and *DNAI2*) and one of the two basal cell markers examined (*p63*), although to a lesser

(B) Primary screen results from human airway basal cells grown in 3D in the presence of the indicated proteins and analyzed for expression levels of the indicated goblet, ciliated, and basal cell markers. Shown is a heatmap of treatments that induced an increase of one or more markers of one cell type by 2-fold or greater, with a concomitant decrease in markers of one or both of the other cell types by 2-fold or greater. Each data point is the signal intensity relative to the median signal of the plate. Note that the treatments induce an increase in a basal cell marker while decreasing goblet and/or ciliated markers or an increase in one or both goblet cell markers while decreasing ciliated and/or basal cell markers.

degree than anti-Notch1. Anti-Notch3 antibodies had a modest inhibitory effect on two of the three goblet cell markers (*MUC5B* and *FOXA3*), while slightly increasing the expression of the basal cell marker *ITGA6* at higher concentrations, without affecting the expression of ciliated cell markers. Together, these data indicate that Notch2, and not Notch1 or Notch3, is required for the basal-cell-fate decision to become a goblet versus a ciliated cell.

We next asked whether blocking Notch2 or Notch3 could prevent goblet cell metaplasia, a hallmark of several airway diseases including asthma, CF, and COPD. Notch2 antibodies inhibited IL-13-driven goblet cell metaplasia in vitro, as measured by cell-type-specific gene expression in 3D bronchospheres (Figure 4D) and immunostaining with cell-type-specific markers in ALI cultures (Figure 4G), whereas Notch3 inhibition had no effect (Figure S5). Moreover, blocking Notch2, but not Notch3, partially restored ciliated cells (Figures 4E, 4G, and S5) without affecting basal cells (Figures 4F and S5), indicating that the effect of IL-13 on basal cell fate requires Notch2 activity. Interestingly, IL-13 treatment had no effect on the expression of the Notch target gene *NRARP* (Figure S5), suggesting that Notch signaling is not increased downstream of IL-13 and that Notch2 plays a permissive, rather than an instructive role, in cytokine-driven goblet cell metaplasia. We also found that Notch2 antibodies at least partially inhibited the alteration in basal-cell-fate decision downstream of a variety of inflammatory cytokines that we identified as driving goblet cell formation in our secretomics screen (Figure 2B), as measured by qPCR for cell-type-specific markers in bronchospheres (Figure 5) and immunostaining for mucins and acetylated alpha-tubulin in ALI cultures (Figure S6), indicating that Notch2 signaling is generally required for goblet cell metaplasia.

### Inhibition of Notch2 Prevents Goblet Cell Metaplasia In Vivo

To examine the effect of Notch2 inhibition on goblet cell metaplasia in vivo, we administered IL-13 intranasally into mice, which induced a goblet cell phenotype (Figures 6B and 6C), as previously reported (Wills-Karp et al., 1998), with or without coadministration of anti-Notch2 antibodies. Expression levels of the Notch target gene *Nrarp* were not modulated in animals treated with IL-13 and were significantly reduced in animals treated with the anti-Notch2 antibody, as measured by quantitative RT-PCR analysis of RNA from whole-lung tissue (Figure 6F), indicating that IL-13 does not directly activate Notch signaling and verifying the inhibitory activity of anti-Notch2 antibodies in vivo. Periodic acid-Schiff (PAS) staining of lung sections revealed that coadministration of anti-Notch2 antibodies completely blocked IL-13-driven goblet cell metaplasia (Figures 6B and 6C). In addition, the number of Foxj1$^+$-ciliated cells was dramatically increased in animals treated with the anti-Notch2 antibody (Figures 6D and 6E). We verified these observations using quantitative RT-PCR analysis of RNA from whole-lung tissue (Figures 6G–6I). We found that coadministration of anti-Notch2 antibodies together with IL-13 suppressed the expression of multiple goblet-cell-specific genes (*Muc5ac*, *Muc5b*, and *Foxa3*), while dramatically increasing the levels of multiple ciliated-cell-specific genes (*Foxj1* and *Dnai2*), relative to animals treated with IL-13 alone. Anti-Notch2 antibody administration also had a slight but significant increase in the basal-cell-specific genes *Trp63* and *Itga6*. Together, these data indicate that Notch2 is required for IL-13-driven goblet cell metaplasia in vitro and in vivo.

We next examined the effects of anti-Notch2 administration in a model of allergic asthma, where mice are chronically exposed to house dust mite (HDM) to induce many of the clinical symptoms seen in humans, including goblet cell metaplasia (Johnson et al., 2004). Similar to the effects seen on IL-13-induced goblet cell metaplasia, anti-Notch2 antibodies profoundly reduced the amount of mucus induced by HDM administration, as measured by the relative area of PAS staining (Figures S7A and S7B), while dramatically increasing the number of Foxj1$^+$-ciliated cells (Figures S7C and S7D).

Finally, we examined whether anti-Notch2 administration could revert an established goblet cell metaplasia phenotype. The experimental design is schematically depicted in Figure 7A. We induced a goblet cell metaplasia phenotype by intranasal administration of IL-13 for 3 days prior to initiating anti-Notch2 antibody treatments. IL-13 administration, with or without anti-Notch2 antibody, was continued for an additional 6 days. The animals were then analyzed 1 day after the final treatment. Reduced expression of the Notch target gene *Nrarp* in the anti-Notch2-antibody-treated animals, as measured by qPCR analysis of RNA from whole-lung tissue, confirmed Notch pathway inhibition (Figure 7F). PAS staining of lung sections, to measure mucus production (Figure 7B), and quantitative RT-PCR analysis of the expression levels of the goblet-cell-specific genes *Muc5ac*, *Muc5b*, and *Foxa3* in RNA from whole-lung tissue (Figure 7G) confirmed that the goblet cell metaplasia phenotype had occurred after 3 days of IL-13 administration and that this phenotype was completely reversed after treatment with the anti-Notch2 antibody (Figures 7B, 7C, and 7G).

## DISCUSSION

Goblet cell metaplasia is a hallmark of several airway diseases, such as asthma, CF, and COPD. The inability to clear the resulting increase in mucus production can ultimately result in mucostasis and death (Hogg et al., 2004; Kuyper et al., 2003; Lange et al., 1998). Several secreted proteins have been demonstrated to increase mucin expression or secretion in tracheal or airway epithelial cells in culture (Adler et al., 1995; Chen et al., 2003; Fujisawa et al., 2009; Gray et al., 2004; Kettle et al., 2010; Levine et al., 1995; Vermeer et al., 2003); however, only IL-13 and the closely related cytokine IL-4, acting through a shared receptor, have been demonstrated to act directly on the airway epithelium to increase the number of goblet cells in vitro and in vivo by altering airway epithelial cell fate (Atherton et al., 2003; Dabbagh et al., 1999; Grünig et al., 1998; Kuperman et al., 2002; Laoukili et al., 2001; Munitz et al., 2008).

In this study, we utilized a 3D culture model of airway epithelial morphogenesis. 3D culture models utilizing cell lines derived from several epithelial tissues, including kidney (MDCK), intestine (Caco-2), and mammary gland (MCF-10A), have been previously described (Debnath et al., 2003; Elia and Lippincott-Schwartz, 2009; Jaffe et al., 2008). Recently, Rock et al. (2009)

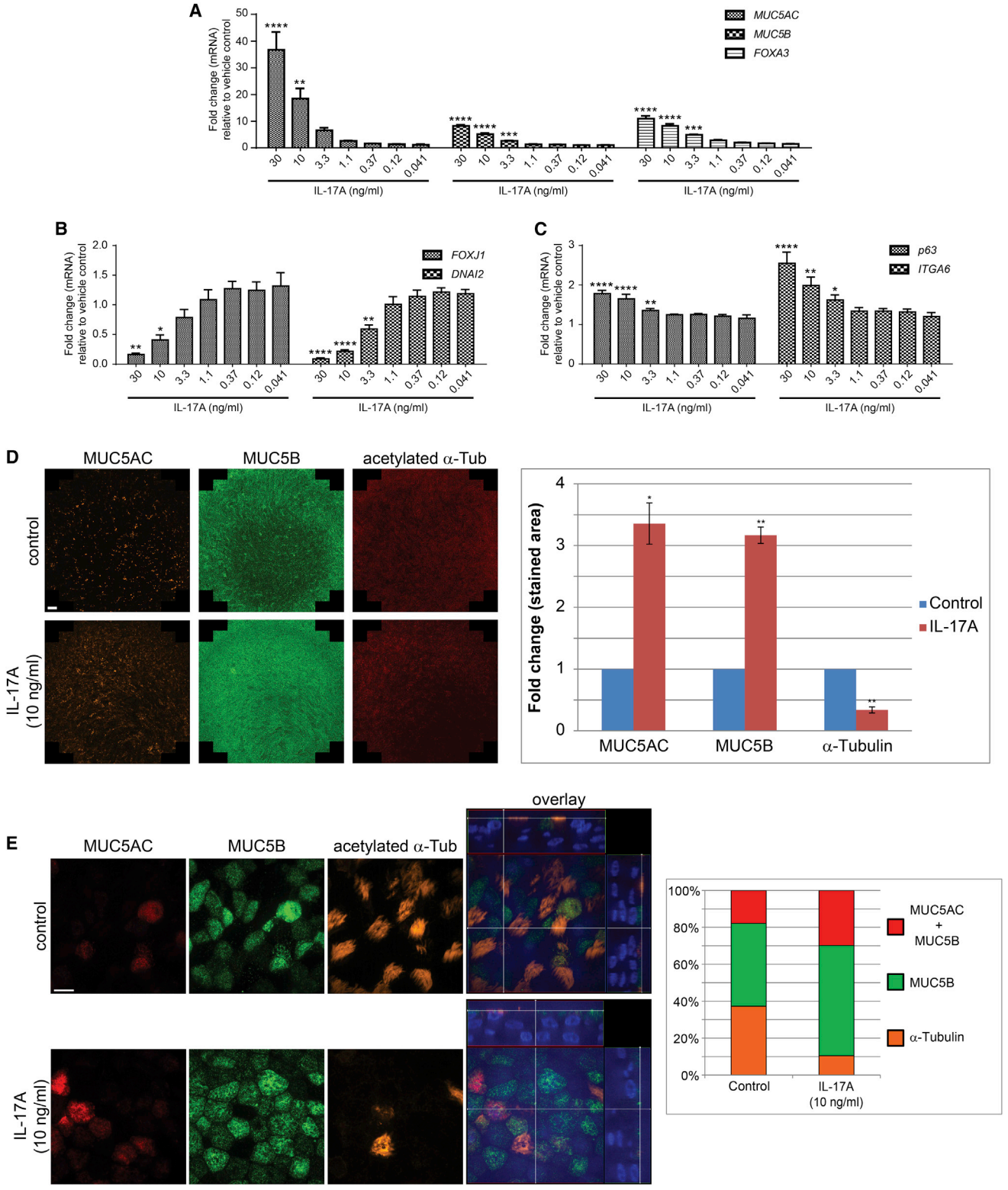


**Figure 3. IL-17A Biases Basal Cell Fate toward a Goblet Cell and away from a Ciliated Cell**

(A–C) Human airway basal cells were grown in 3D to produce bronchospheres, in the presence of increasing concentrations of IL-17A, and analyzed for expression levels of the indicated goblet cell markers (A), ciliated cell markers (B), and basal cell markers (C). Shown is the mean fold change ± SEM relative to control from three independent experiments (n = 3). *p < 0.05; **p < 0.01; ***p < 0.001; ****p < 0.0001. One-way ANOVA and Dunnett's multiple comparison test.

*(legend continued on next page)*

described the formation of ''tracheospheres'' from either Krt5$^+$ murine basal cells or ITGA6$^+$NGFR$^+$ human basal cells in 3D Matrigel-based culture. Tracheospheres contained a central lumen surrounded by ciliated cells but lacked detectable MUC5AC$^+$ secretory cells (Rock et al., 2009). Wu et al. (2010) also reported the formation of polarized 3D structures in Matrigel that were derived from surface epithelial HBE cells (Wu et al., 2011). These structures that were cultured on four chamber slides were termed ''glandular acinar'' cells based upon the expression of MUC5B and the lack of ciliated cells (Wu et al., 2011). Whereas each of these systems recapitulates some aspects of the architecture of the conducting airway, neither captures the full diversity of cell types found in this region of the respiratory tract. In particular, there are no reported 3D culture systems that contain an airway progenitor cell, mucus-producing secretory cells, and ciliated cells. The bronchospheres described in this study derive from multipotent p63$^+$NGFR$^+$ITGA6$^+$ airway basal cell, a progenitor cell for the human conducting epithelium, and recapitulate key elements of the conducting airway epithelium, including a pseudostratified epithelium containing basal cell progenitors, mucus-secreting goblet cells, and ciliated cells, surrounding a single central lumen.

We scaled the 3D bronchosphere system to a 384-well plate format to allow for much higher throughput screening and analyses when compared with the widely used ALI cultures of primary epithelia (Gray et al., 1996). We used this system to screen a library of secreted proteins (Gonzalez et al., 2010) and found a number of factors that modulated basal cell fate, as judged by a decrease in one or more cell-type-specific markers with a concomitant increase in one or more markers of another cell type. One group of treatments drove an increase in a basal cell marker and a decrease in one or more markers of ciliated cells and/or goblet cells, consistent with inhibition of differentiation. Interestingly, these proteins were almost exclusively members of the epidermal growth factor family of ligands. A recent study found that EGF receptor is expressed by human airway basal cells, and is activated by smoke-induced EGF expression in ciliated cells to prevent basal cell differentiation into ciliated and goblet cells and drive a squamous metaplasia phenotype (Shaykhiev et al., 2013). Our data suggest that other EGF ligands may have a similar activity and could play a role in driving squamous metaplasia in other settings.

The second type of effect that we observed on basal cell fate was an increase in one or more of the goblet cell markers and a decrease in one or more ciliated or basal cell markers. More than half of the proteins that biased cell fate toward a goblet cell were inflammatory cytokines. This has several implications for the treatment of airway diseases. First, it provides a rationale for the development of cytokine-specific therapies and stratifying patients based on either levels of a particular cytokine or a biomarker indicating activation of a pathway downstream of a particular cytokine. The increased response in asthma patients with higher levels of periostin in recent clinical trials with anti-IL-13 antibodies supports this idea (Corren et al., 2011). Second, it suggests that treatments designed to inhibit the production or secretion of mucus from goblet cells may not be sufficient, because they may not restore the appropriate numbers of ciliated cells required for adequate mucociliary clearance. Finally, although the factors we found to influence basal cell fate activate distinct signaling pathways, their similar effect on a cellular process, biasing progenitor cell fate toward a goblet cell and away from a ciliated cell, suggested that there may be a common druggable node that would have therapeutic benefit for patients with a wide range of underlying causes.

Notch signaling is an evolutionarily conserved pathway that regulates many cell-fate decisions during development (Fortini, 2009). Mammalian cells contain four Notch receptors (Notch 1–Notch 4), which are activated by membrane-bound ligands, members of the Delta and Jagged family, on neighboring cells. Notch activation leads to a series of cleavage events, culminating in the generation of the Notch intracellular domain (NICD), which translocates to the nucleus, where it interacts with a transcription factor complex to regulate gene expression. The role of Notch signaling in regulating cell-fate decisions during development and repair has been studied in many contexts, including in mucociliary tissues (Deblandre et al., 1999; Guseh et al., 2009; Morimoto et al., 2010, 2012; Rock et al., 2011; Tsao et al., 2009). In the epidermis of the *Xenopus* embryo, activation of Notch suppresses the ciliated cell fate, whereas inhibition of Notch signaling results in an overproduction of ciliated cells (Deblandre et al., 1999). In the developing mouse airway, expression of the NICD results in an overproduction of secretory cells at the expense of ciliated cells (Guseh et al., 2009), whereas deletion of *Pofut1*, an O-fucosyltransferase required for Notch-ligand interactions (Stahl et al., 2008), or *Rbpjk*, a core nuclear effector of Notch signaling (Fortini, 2009), results in an increase in the number of ciliated cells and a near absence of secretory cells (Tsao et al., 2009). A recent study using Notch-receptor-specific knockouts suggested that *Notch2* is the critical Notch receptor regulating secretory versus ciliated cell fate in the mouse developing airway (Morimoto et al., 2012).

We found that Notch2 acts as a common node downstream of IL-13, as well as the mediators of goblet cell metaplasia identified in this study. Antibodies that specifically inhibit Notch2, but not other Notch receptor family members Notch1 and Notch3, inhibit IL-13-driven goblet cell metaplasia in vitro, and administration of anti-Notch2 antibodies prevented IL-13 as well as allergen-driven goblet cell metaplasia in vivo. Moreover,

(D) Human airway basal cells were grown on filters at air-liquid interface with or without IL-17A (10 ng/ml). Shown are representative tiled images of control (top row) and IL-17A-treated (bottom row) filters stained for MUC5AC (orange), MUC5B (green), and acetylated $\alpha$-tubulin (red). The scale bar represents 500 $\mu$m. Quantification of the total staining area for each marker is shown to the right. Shown is the average fold change $\pm$ SEM relative to control from three independent experiments, each performed in duplicate. *$p < 0.01$; **$p < 0.001$. Paired, two-tailed Student's t test.

(E) Representative confocal sections of control (top) and IL-17A-treated (bottom) filters stained for MUC5AC (red), MUC5B (green), acetylated $\alpha$-tubulin (orange), and DNA (blue). The scale bar represents 10 $\mu$m. Quantification of the number of cells staining positive for each marker is shown to the right. Quantification was performed with four independent regions of each filter from the experiments shown in (D). A total of more than 700 cells were counted from control and IL-17A-treated filters, respectively. Shown is the percentage of cells stained for each marker.

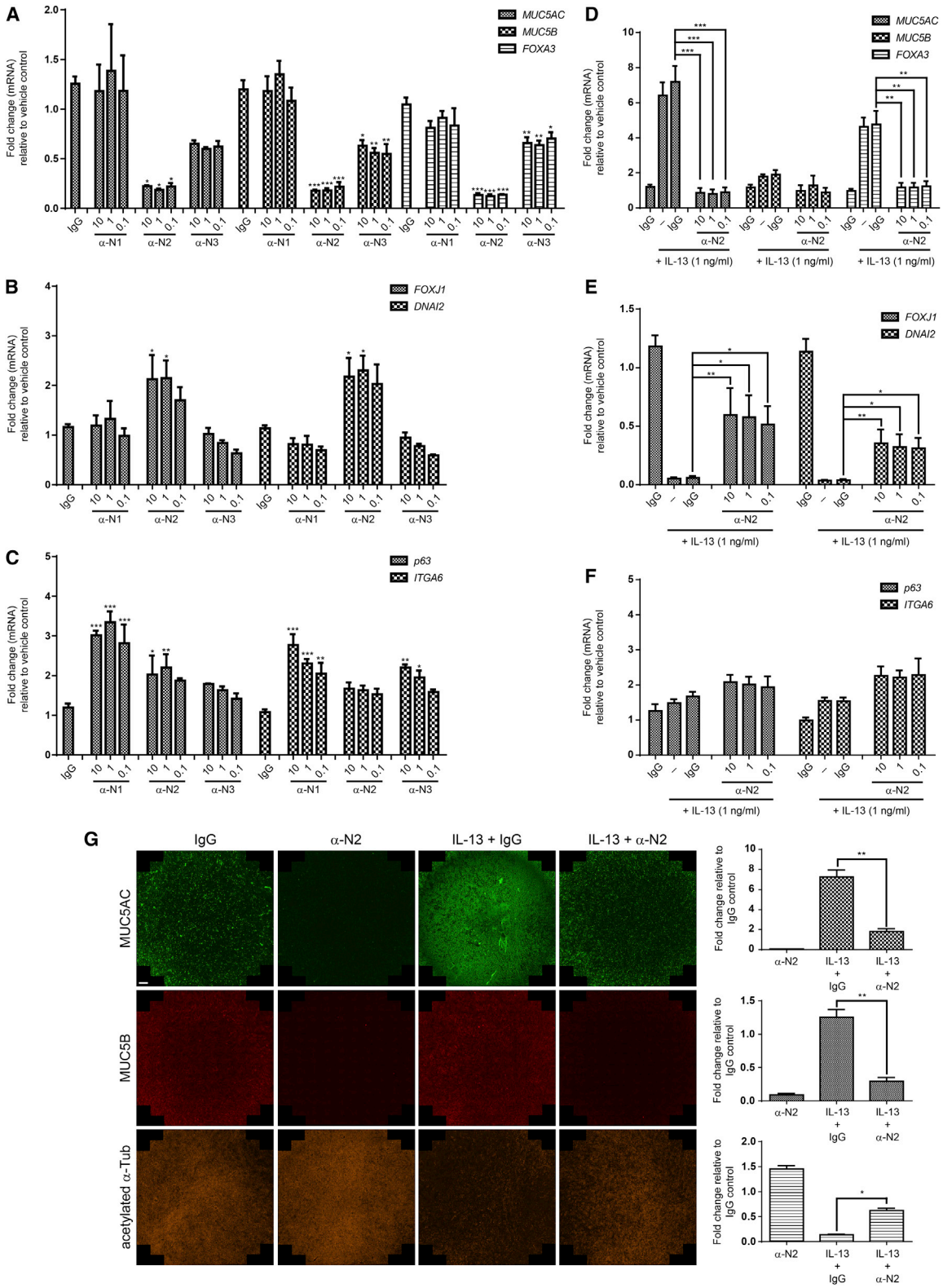


**Figure 4. Notch2 Inhibition Alters Cell Fate away from a Goblet Cell and toward a Ciliated Cell**

(A–C) Human airway basal cells were grown in 3D to produce bronchospheres, in the presence of vehicle control; IgG (10 μg/ml); or increasing concentrations (μg/ml) of inhibitory antibodies specific for Notch1 (α-N1), Notch2 (α-N2), or Notch3 (α-N3), and analyzed for the expression levels of the indicated goblet cell

*(legend continued on next page)*

Notch2 antibodies prevented the changes in basal cell fate driven by multiple cytokines in our 3D bronchosphere system and in ALI cultures, including cytokines that are increased in patients with asthma, COPD, or both, which have been proposed to play a role in these diseases (Barnes, 2008). Finally, we found that administration of anti-Notch2 antibodies reversed a pre-established goblet cell metaplasia phenotype in vivo. Collectively, our data support the use of Notch2-specific inhibitors in the treatment of airway diseases with goblet cell metaplasia, regardless of the disease stimulus.

## EXPERIMENTAL PROCEDURES

### Antibodies and Reagents

Primary antibodies used in this study were MUC5AC (clone 45M1; Thermo Scientific), acetylated α-tubulin (clone 6-11B-1; Sigma-Aldrich), mouse anti-p63 (clone 4A4; Santa Cruz Biotechnology), rabbit anti-p63 (Abcam), ITGA6 (Go H3; Abcam), NGFR (Abcam), Ki-67 (Invitrogen), and FOXJ1 (HPA005714; Sigma). Alexa 488, Alexa Fluor 568, and Alexa Fluor 633 secondary antibodies, Alexa Fluor 647 and rhodamine-conjugated phalloidin, Oregon Green 488 carboxylic acid diacetate (carboxy-DFFDA), and ProLong gold antifade with DAPI were obtained from Invitrogen.

### Tissue Culture

Human airway basal cells (sold as "normal human bronchial/tracheal epithelial cells") and culture media were obtained from Lonza. All cells purchased from Lonza were from normal donors, ranging in age from 3 to 60 years old. Air-liquid interface cultures using passage 2 (P2) cells were performed as previously described (Danahay et al., 2002). At this passage, these cells retain the ability to differentiate into a mucociliary epithelium at ALI, whereas at higher passages (>4), the cells lose this ability (Araya et al., 2007; Gray et al., 1996). For 3D culturing of airway basal cells, P1 cells were trypsinized and resuspended (30,000 cells/ml) in HBE differentiation media containing 5%-growth-factor-reduced Matrigel (BD Biosciences). Twenty microliters of suspension was plated in each well of a 384-well plate (Greiner) precoated with 10 μl of a 25% solution of Matrigel (BD Biosciences) in HBE differentiation media. Wells were fed or treated at day 2 and day 8 of culture by adding 30 μl of differentiation media containing the appropriate treatment. 3D cultures were analyzed at the time points indicated. For the cell-mixing experiments to determine the seeding density for deriving clonal bronchospheres, airway basal cells were labeled with carboxy-DFFDA and mixed with unlabeled HBE cells at a 1:1 ratio prior to plating in 3D in 384-well plates.

For screening studies of 3D bronchosphere cultures, P1 cells and 384-well plates were prepared and treated in duplicate with a collection of 4,876 secreted, recombinant human proteins representing the predicted human "secretome" (Gonzalez et al., 2010), essentially as described above. To automate the process, a Wellmate (Thermo Scientific) microplate dispenser was used to plate cells and a Biomek FXP 384-multichannel pipetting head (Beckman Coulter) was used to precoat, feed, and treat wells. Protein and control samples suspended in Tris-buffered saline buffer were arrayed in 384-well v-bottom plates (Greiner). Samples were diluted to a working concentration in assay media with 0.1% BSA (Sigma) and were then used to treat wells at day 2 and day 8 of culture at a final concentration of 4.4 nM–1.24 μM (indicated in Table S1), depending on the sample protein. To record 3D structure morphology, a bright-field image of each well was taken on day 12 of culture using an IN Cell Analyzer 2000 high-content imaging system (GE Healthcare Life Sciences). Gene expression was quantified on day 14 of culture using the QuantiGene Plex 2.0 Assay (Affymetrix).

### QuantiGene 2.0 Multiplex Assays

To quantify gene expression of 3D bronchosphere cultures, the QuantiGene 2.0 Multiplex Assay (Affymetrix) was used. All sample transfers were done with a Biomek FXP 384-multichannel pipetting head (Beckman Coulter). Solution additions were done with a Wellmate microplate dispenser (Thermo Scientific). Wells were aspirated and washed with an ELX406 plate washer (BioTek). RNA was processed with the QuantiGene Sample Processing kit (Affymetrix) according to the manufacturer's specifications. Briefly, day 14 bronchosphere plates (384-well) were aspirated to 30 μl and 15 μl of Panomics Lysis mixture was added. A 40 μl sample of each well was transferred to a 384-well v-bottom plate (Greiner), and 20 μl of a hybridization solution containing lysis mixture, proteinase k, blocking reagent, a probe set, and a bead set was added to each well. To hybridize RNA, probes, and beads, plates were sealed and incubated at 55°C overnight in an orbital shaking incubator at 500 rpm (Liconic). The probe set containing the following target genes: *POLR2A* (NM_000937); *ITGA6* (NM_001079818); *MUC5B* (NM_002458); *MUC5AC* (NM_017511); *p63* (NM_003722); *DNAI2* (NM_023036); and *FOXJ1* (NM_001454) is available from Affymetrix (panel 11783/catalog no. 311783). The next day, wash solution, preamplifier solution, amplifier solution, and label probe streptavidin-phycoerythrin (SAPE) solution were prepared using the manufacturer's specifications. Hybridized RNA was multiplexed by combining in a clear, flat-bottom, 384-well plate (Nunc). The plate was placed on a magnetic holder, and wells were washed three times. RNA was incubated for 1 hr at 50°C and 500 rpm with preamplifier solution and then washed as before. This incubation and wash cycle was repeated for addition of amplifier solution and again for label probe SAPE solution. A bead-suspending solution was added, and each well was then read using the Flexmap 3D instrument (Luminex). RNA quality was monitored by examining the signal for a housekeeper (*POLR2A*) to ensure that the levels were similar to other wells. The effect of each of the recombinant proteins screened was determined by calculating the average (n = 2 replicates for the screen) of the median signal of a well relative to the median signal of the plate (excluding active control wells) for each probe (i.e., for each target gene).

### Microscopy

Immunofluorescence of 3D bronchospheres was performed as described previously for MCF10A cysts (Debnath et al., 2003) with the following modifications. After incubation with fluorescence-conjugated secondary antibodies, DNA was stained with a 1:1 mix of PBS and ProLong gold antifade containing DAPI. Confocal microscopy was performed at room temperature on a microscope (Zeiss LSM510 Meta) using an EC Plan-Neofluar 10×/0.30 dry objective (Zeiss), an EC Plan-Neofluor 20×/0.5 dry objective (Zeiss), a C-Apochromat 40×/1.2 W corr (Zeiss), or a C-Apochromat 63×/1.2 W Corr objective (Zeiss). Images were collected with Zen confocal software (Zeiss). Scale bars were added, and images were processed using Zen (Zeiss) and Photoshop (Adobe). ALI cultures were processed for immunofluorescence analysis

markers (A), ciliated cell markers (B), and basal cell markers (C). Shown is the mean fold change ± SEM relative to control from at least three independent experiments. *p < 0.05; **p < 0.01; ***p < 0.001. One-way ANOVA and Dunnett's multiple comparison test.

(D–F) Human airway basal cells were grown in 3D to produce bronchospheres, in the presence of vehicle control or IgG (10 μg/ml), with or without 1 ng/ml IL-13, or increasing concentrations of α-N2 (μg/ml) together with 1 ng/ml of IL-13, and analyzed for the expression levels of the indicated goblet cell markers (D), ciliated cell markers (E), and basal cell markers (F). Shown is the mean fold change ± SEM relative to control from at least four independent experiments. *p < 0.05; **p < 0.01; ***p < 0.001. One-way ANOVA and Dunnett's multiple comparison test.

(G) Representative tiled images of ALI cultures treated with IgG control (first column), α-N2 (second column), 1 ng/ml IL-13 + IgG control (third column), or 1 ng/ml IL-13 + α-N2 (fourth column) and stained for MUC5AC (green), MUC5B (red), and acetylated α-tubulin (orange). The scale bar represents 500 μm. Quantification of the total staining area for each marker is on the right. Shown is the average fold change ± SEM relative to control from three independent experiments, each with five filters per treatment. Note that α-N2 inhibits the IL-13-driven increase in MUC5AC staining and partially restores levels of acetylated α-tubulin. *p < 0.01; **p < 0.001. Paired, two-tailed Student's t test.

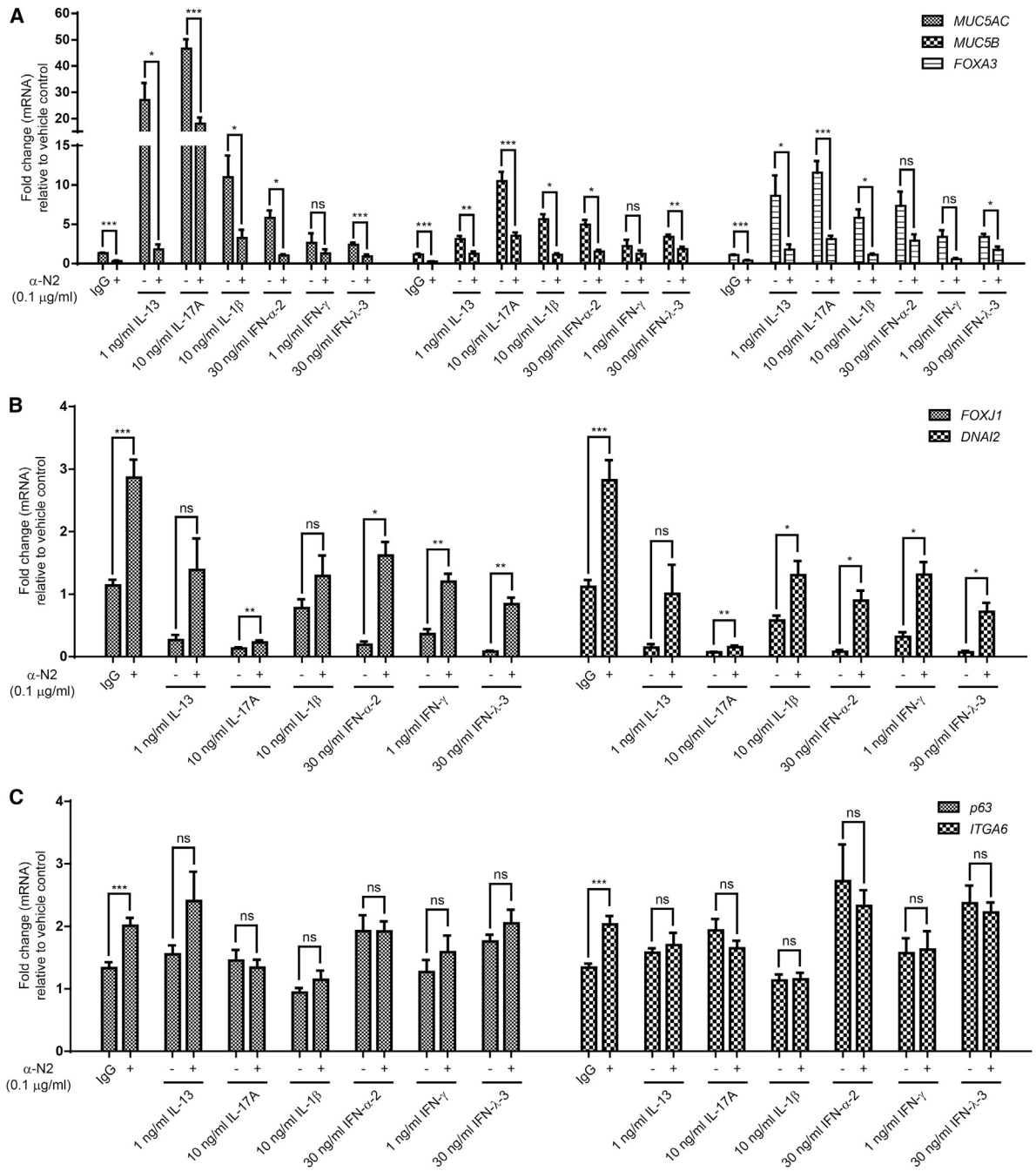


**Figure 5. Notch2 Inhibition Blocks Goblet Cell Metaplasia Downstream of Multiple Mediators**

Human airway basal cells were grown in 3D to produce bronchospheres, in the presence of IgG (0.1 μg/ml) or α-N2 (0.1 μg/ml), together with the indicated proteins, and analyzed for the expression levels of goblet cell markers (A), ciliated cell markers (B), and basal cell markers (C). Shown is the mean fold change ± SEM relative to control from at least three independent experiments. *p < 0.05; **p < 0.01; ***p < 0.001; ns, not significant. Paired, two-tailed Student's t test.

after 14 days of culture at ALI by rinsing the apical surface of each filter with PBS and then fixing in 4% paraformaldehyde for 4 hr. Filters were washed with IF buffer (130 mM NaCl, 7 mM Na2HPO4, 3.5 mM NaH2PO4, 7.7 mM NaN3, 0.1% bovine serum albumin, 0.2% Triton X-100, and 0.05% Tween-20), blocked with IF wash containing 10% goat serum, and stained with primary antibody in IF wash containing 10% goat serum overnight at 4°C. Secondary antibodies were used at a 1:200 dilution in IF buffer containing 10% goat serum. To quantify the total staining area of ALI cultures, 10 × 13 images were collected with a plan Neofluar 10× 0.3 numerical aperture (NA) Ph1 objective (EC; Carl Zeiss) on a microscope (Axiovert 200; Carl Zeiss) equipped with a motorized stage and a camera (Orca-ER-1394; Hamamatsu Photonics) controlled by Axiovision software (Carl Zeiss) and used to generate a single composite image using the MOSAIX function in Zeiss Axiovision. Quantification of the total staining area was performed with ImageJ.

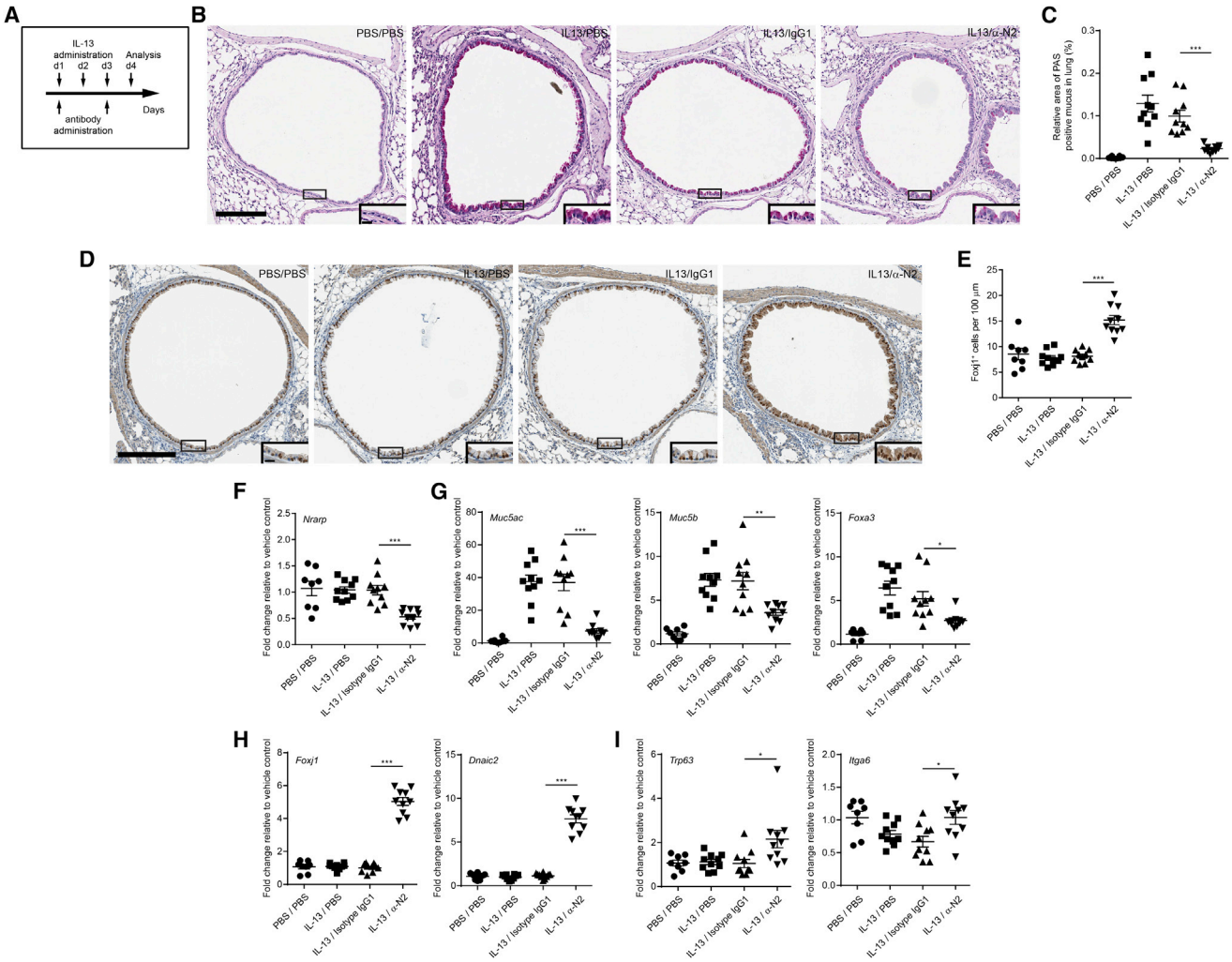


**Figure 6. Notch2 Neutralization Inhibits IL-13-Driven Goblet Cell Metaplasia In Vivo**

(A) Schematic representation of the experimental design.

(B) Representative images of PAS-stained lung sections from the indicated treatment groups (8–10 mice per group). PAS positivity is dark violet. The scale bar represents 200 μm. The inset scale bar represents 20 μm.

(C) Quantification of the relative area of PAS staining in the lung. Shown is the mean ± SEM. Each dot represents one mouse.

(D) Representative images of lung sections from the indicated treatment groups (8–10 mice per group) stained for the ciliated-cell-specific marker Foxj1. The scale bar represents 200 μm. The inset scale bar represents 20 μm.

(E) Quantification of the number of Foxj1$^+$ cells per 100 μm of epithelium. Shown is the mean ± SEM. Each dot represents one mouse.

(F) Quantitative PCR analysis of the Notch target gene *Nrarp* in lungs from the indicated treatment groups.

(G–I) Quantitative PCR analysis of goblet (*Muc5ac*, *Muc5b*, and *Foxa3*; G), ciliated (*Foxj1* and *Dnaic2*; H), and basal cell marker (*Trp63* and *Itga6*; I) expression in lungs from the indicated treatment groups. Shown is the mean fold change ± SEM relative to control. Each dot represents one mouse. *$p < 0.05$; **$p < 0.01$; ***$p < 0.001$. One-way ANOVA and Dunnett's multiple comparison test.

Two to three regions of each ALI culture were punched out with a 4 mm biopsy punch (Miltex) and mounted in ProLong gold antifade containing DAPI for imaging by confocal microscopy on a microscope (Axiovert 200; Carl Zeiss) equipped with a motorized stage, a Yokogawa CSU-X1 spinning disc head, and an electron-multiplying charge-coupled device camera (Evolve 512; Photometrics), with a Plan-Apochromat 100×/1.4 oil differential interference contrast (DIC) objective (Zeiss). Cells positive for MUC5AC, MUC5B, or cilia (acetylated α-tubulin) staining were counted manually. For time-lapse video microscopy, human bronchial epithelial cells were imaged at the indicated times during bronchosphere development at 37°C with a plan Neofluar 10× 0.3 NA Ph1 objective (EC; Carl Zeiss). Images were taken every 5 min for the indicated time period. Annotations (time stamp and scale bar) were added, and videos were assembled using Axiovision software.

### RNA Isolation and Quantitative PCR

RNA was isolated from 3D bronchosphere cultures with Trizol (Invitrogen), using manufacturer's specifications. To isolate RNA from mouse tissue, approximately 20 mg of tissue was placed in a 1.5 ml Eppendorf tube with 1 ml of Buffer RLT Plus (QIAGEN) containing 10 μl of 2-mercaptoethanol (Sigma). A 5 mm stainless steel bead (QIAGEN) was added to the tube, and the tissue was sheared using a Tissue Lyser II (QIAGEN). RNA from the sheared tissue was purified using the RNeasy Plus Mini Kit (QIAGEN), using manufacturer's

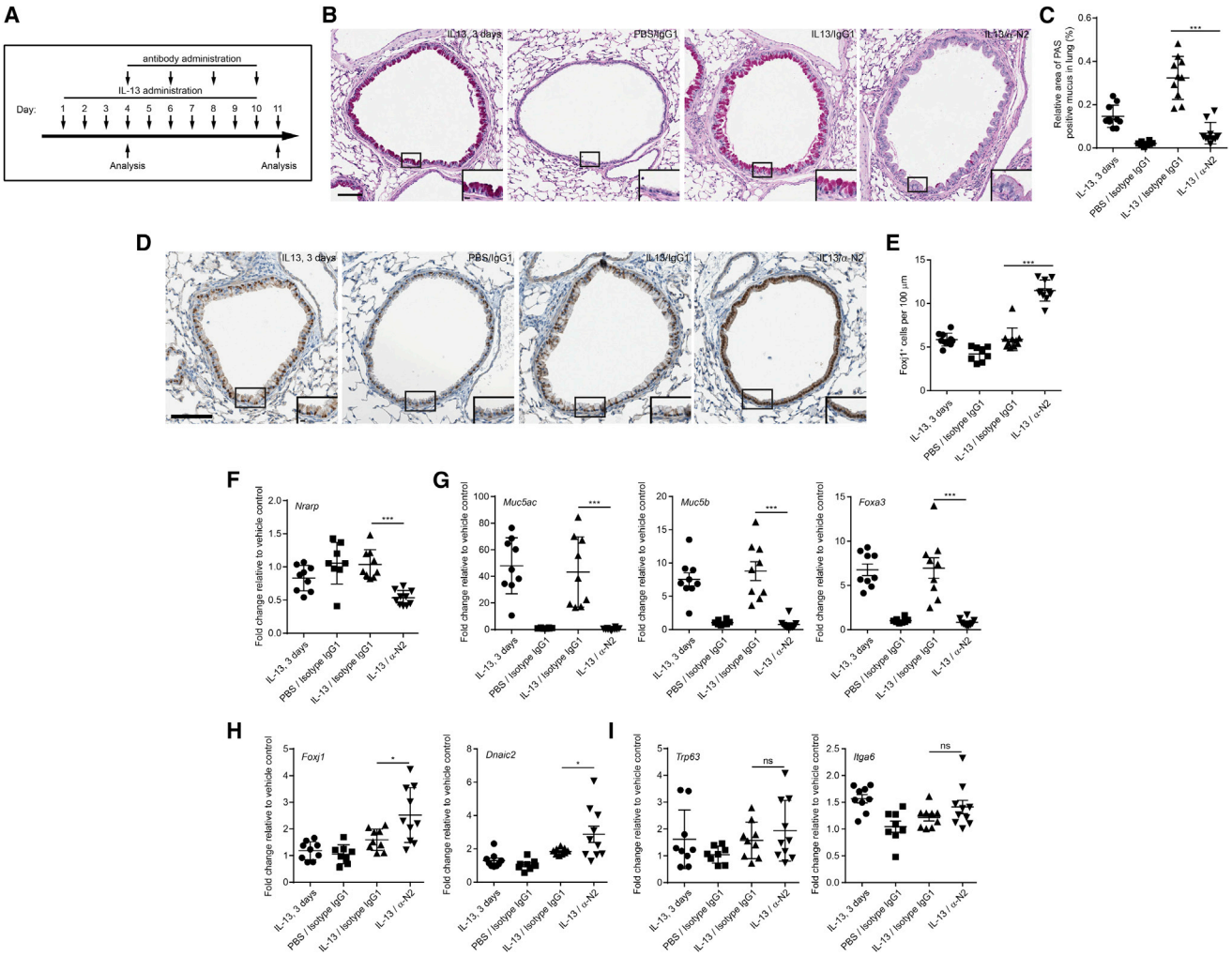


**Figure 7. Notch2 Neutralization Reverts a Preexisting IL-13-Induced Goblet Cell Metaplasia In Vivo**

(A) Schematic representation of the experimental design.

(B) Representative images of PAS-stained lung sections from the indicated treatment groups (8–10 mice per group). PAS positivity is dark violet. The scale bar represents 100 μm. The inset scale bar represents 10 μm.

(C) Quantification of the relative area of PAS staining in the lung. Shown is the mean ± SEM. Each dot represents one mouse.

(D) Representative images of lung sections from the indicated treatment groups (8–10 mice per group) stained for the ciliated-cell-specific marker Foxj1. The scale bar represents 100 μm. The inset scale bar represents 10 μm.

(E) Quantification of the number of Foxj1$^+$ cells per 100 μm of epithelium. Shown is the mean ± SEM. Each dot represents one mouse.

(F–H) Quantitative PCR analysis of goblet (*Muc5ac*, *Muc5b*, and *Foxa3*; F), ciliated (*Foxj1* and *Dnaic2*; G), and basal cell marker (*Trp63* and *Itga6*; H) expression in lungs from the indicated treatment groups.

(I) Quantitative PCR analysis of the Notch target gene *Nrarp* in lungs from the indicated treatment groups. Shown is the mean fold change ± SEM relative to control. Each dot represents one mouse. *p < 0.05; ***p < 0.001; ns, not significant. One-way ANOVA and Dunnett's multiple comparison test.

specifications. TaqMan Reverse Transcription Reagents (Invitrogen) were used to generate cDNA from 1 μg of total RNA. Quantitative PCR was performed on a ViiA7 Real-Time PCR System (Applied Biosystems), using 40 ng of cDNA per reaction with the following Taqman probes (Applied Biosystems): *MUC5AC*, Hs01365601_m1; *MUC5B*, Hs00861588_m1; *FOXA3*, Hs00270130_m1; *FOXJ1*, Hs00230964_m1; *DNAI2*, Hs01001544_m1; *p63*, Hs00978340_m1; *ITGA6*, Hs01041011_m1; *NOTCH1*, Hs01062011_m1; *NOTCH2*, Hs01050702_m1; *NOTCH3*, Hs01128541_m1; *NOTCH4*, Hs00965897_m1; *HEY1*, Hs01114113_m1; *HEY2*, Hs00232622_m1; *HES1*, Hs00172878_m1; *HES5*, Hs01387463_g1; *NRARP*, Hs01104102_s1; *GAPDH*, Hs99999905_m1; *Muc5ac*, Mm012718_m1; *Foxj1*, Mm012367279_m1; *Trp63*, Mm00495788_m1; and *Gapdh*, Mm99999915_g1.

## Animal Models

Female Balb/c mice (20–25 g) were obtained from Charles River Laboratories. Mice were housed under specific pathogen-free conditions and were provided with food and water ad libitum. Experiments were performed in accordance with the UK Animals Scientific Procedures Act 1986.

For the experiment shown in Figure 6, mice received 0.5 μg of recombinant mouse IL-13 (Ebiosciences) or PBS intranasally on 3 consecutive days (days 1–3). Mice received either 20 mg/kg neutralizing antibody to Notch2 or control immunoglobulin G (IgG) or PBS intraperitoneally 2 hr before intranasal challenge with either IL-13 or PBS on days 1 and 3 only. Mice were euthanized 24 hr after the final IL-13 administration.

For the experiment shown in Figure S7 (chronic house dust mite model), mice received 25 μg of HDM (*D. pteronyssinus*; GREER Laboratories) or saline intranasally on 5 days a week for 5 weeks (days 1–5, 8–12, 15–19, 22–26, and 29–31). Mice received either 20 mg/kg neutralizing anti-Notch2 antibody or isotype control IgG intraperitoneally 2 hr before intranasal challenge with HDM on days 22, 24, 26, 28, and 30 only. Mice were euthanized 24 hr after their final saline or HDM administration (day 32).

For the experiment shown in Figure 7, mice received 0.5 μg of recombinant mouse IL-13 (Ebiosciences) or PBS intranasally on 10 consecutive days (days 1–10). Mice received either 20 mg/kg neutralizing anti-Notch2 antibody or isotype control IgG intraperitoneally 2 hr before intranasal challenge with either IL-13 or PBS on days 4, 6, 8, and 10 only. An additional group of mice received 0.5 μg of recombinant mouse IL-13 (Ebiosciences) or PBS intranasally on 3 consecutive days (days 1–3) only. Mice were euthanized 24 hr after their final PBS or IL-13 administration.

The left lungs were excised, inflated with 10% neutral buffered formalin (NBF), and preserved in NBF. Lungs were embedded in paraffin wax and lung sections obtained for each animal. Sections were stained with PAS stain for mucus and with anti-Foxj1 antibodies (Sigma) to label ciliated cells.

PAS-positive staining and Foxj1-positive nuclei were quantified in lung sections using Definiens Image Analysis software. Two distinct lung sections were analyzed per mouse, and the total area of PAS-positive staining or the number of Foxj1-positive nuclei within the sections was determined. The PAS-positive staining was normalized to the area of tissue analyzed and represented as "relative area PAS-positive mucus (%)". The Foxj1-positive nuclei are represented as "$Foxj1^+$ cells per 100 μm" of epithelium.

Data are expressed as mean ± SEM. Statistical significance was determined using a parametric one-way ANOVA and Dunnett's posttest. GraphPad Prism (version 5.04) was used to generate graphs and perform statistical analysis. ***$p < 0.001$ denotes statistically significant difference from relevant isotype control group.

Additional methods are provided in the Supplemental Experimental Procedures.

## SUPPLEMENTAL INFORMATION

Supplemental Information includes Supplemental Experimental Procedures, seven figures, one table, and four movies and can be found with this article online at http://dx.doi.org/10.1016/j.celrep.2014.12.017.

## AUTHOR CONTRIBUTIONS

H.D. and A.B.J. conceived the project. H.D., A.D.P., J.C., B.E.M., D.X., A.W., H.Y., Z.W., L.B., C.T., S.P., G.L.V.-R., M.E., P.C., A.C., M.H., and A.B.J. designed and performed the experiments. H.D., A.D.P., J.C., B.E.M., D.X., A.W., H.Y., Z.W., L.B., C.T., S.P., A.D., G.L.V.-R., M.E., P.C., A.C., M.H., and A.B.J. analyzed the results. A.L., P.L., P.B., and C.J.F. provided new reagents. H.D. and A.B.J. wrote the manuscript.

## ACKNOWLEDGMENTS

We thank the members of the A.B.J. and H.D. labs, as well as Somnath Bandyopadhyay, Bob Strieter, Jonathan Arm, Leon Murphy, and members of the Murphy lab and the Regenerative Medicine Hub for helpful discussions; John Wailes (Zeiss) for help and advice on image acquisition and analysis; Alan Abrams for generating the graphical abstract and help with time-lapse movie formatting; and Ralph J. DeBerardinis, Beat Nyfeler, Rob McDonald, and John Hastewell for critical review of the manuscript. We would also like to thank Tewis Bouwmeester, Pete Finan, Martin Gosling, Mark Labow, Vic Myer, Jeff Porter, and John Westwick for support and input throughout the course of this work. H.D, A.D.P., J.C., B.E.M., D.X., A.W., H.Y., Z.W., L.B., C.T., S.P., A.L., P.L., A.D., G.L.V.-R., P.B., C.J.F., M.E., P.C., A.C., M.H., and A.B.J. are employees of Novartis, as indicated in the affiliations.

Received: October 22, 2013
Revised: October 3, 2014
Accepted: December 9, 2014
Published: December 31, 2014

## REFERENCES

Adler, K.B., Fischer, B.M., Li, H., Choe, N.H., and Wright, D.T. (1995). Hypersecretion of mucin in response to inflammatory mediators by guinea pig tracheal epithelial cells in vitro is blocked by inhibition of nitric oxide synthase. Am. J. Respir. Cell Mol. Biol. *13*, 526–530.

Araya, J., Cambier, S., Markovics, J.A., Wolters, P., Jablons, D., Hill, A., Finkbeiner, W., Jones, K., Broaddus, V.C., Sheppard, D., et al. (2007). Squamous metaplasia amplifies pathologic epithelial-mesenchymal interactions in COPD patients. J. Clin. Invest. *117*, 3551–3562.

Atherton, H.C., Jones, G., and Danahay, H. (2003). IL-13-induced changes in the goblet cell density of human bronchial epithelial cell cultures: MAP kinase and phosphatidylinositol 3-kinase regulation. Am. J. Physiol. Lung Cell. Mol. Physiol. *285*, L730–L739.

Barnes, P.J. (2008). The cytokine network in asthma and chronic obstructive pulmonary disease. J. Clin. Invest. *118*, 3546–3556.

Bray, S., and Bernard, F. (2010). Notch targets and their regulation. Curr. Top. Dev. Biol. *92*, 253–275.

Chen, Y., Thai, P., Zhao, Y.H., Ho, Y.S., DeSouza, M.M., and Wu, R. (2003). Stimulation of airway mucin gene expression by interleukin (IL)-17 through IL-6 paracrine/autocrine loop. J. Biol. Chem. *278*, 17036–17043.

Chesné, J., Braza, F., Mahay, G., Brouard, S., Aronica, M., and Magnan, A. (2014). IL-17 in Severe Asthma. Where Do We Stand? Am. J. Respir. Crit. Care Med. *190*, 1094–1101.

Corren, J., Lemanske, R.F., Hanania, N.A., Korenblat, P.E., Parsey, M.V., Arron, J.R., Harris, J.M., Scheerens, H., Wu, L.C., Su, Z., et al. (2011). Lebrikizumab treatment in adults with asthma. N. Engl. J. Med. *365*, 1088–1098.

Dabbagh, K., Takeyama, K., Lee, H.M., Ueki, I.F., Lausier, J.A., and Nadel, J.A. (1999). IL-4 induces mucin gene expression and goblet cell metaplasia in vitro and in vivo. J. Immunol. *162*, 6233–6237.

Danahay, H., Atherton, H., Jones, G., Bridges, R.J., and Poll, C.T. (2002). Interleukin-13 induces a hypersecretory ion transport phenotype in human bronchial epithelial cells. Am. J. Physiol. Lung Cell. Mol. Physiol. *282*, L226–L236.

Deblandre, G.A., Wettstein, D.A., Koyano-Nakagawa, N., and Kintner, C. (1999). A two-step mechanism generates the spacing pattern of the ciliated cells in the skin of Xenopus embryos. Development *126*, 4715–4728.

Debnath, J., Muthuswamy, S.K., and Brugge, J.S. (2003). Morphogenesis and oncogenesis of MCF-10A mammary epithelial acini grown in three-dimensional basement membrane cultures. Methods *30*, 256–268.

Elia, N., and Lippincott-Schwartz, J. (2009). Culturing MDCK cells in three dimensions for analyzing intracellular dynamics. Curr. Protoc. Cell Biol. *Chapter 4*, Unit 4.22.

Fahy, J.V., and Dickey, B.F. (2010). Airway mucus function and dysfunction. N. Engl. J. Med. *363*, 2233–2247.

Finkelman, F.D., Hogan, S.P., Hershey, G.K., Rothenberg, M.E., and Wills-Karp, M. (2010). Importance of cytokines in murine allergic airway disease and human asthma. J. Immunol. *184*, 1663–1674.

Fortini, M.E. (2009). Notch signaling: the core pathway and its posttranslational regulation. Dev. Cell *16*, 633–647.

Fujisawa, T., Velichko, S., Thai, P., Hung, L.Y., Huang, F., and Wu, R. (2009). Regulation of airway MUC5AC expression by IL-1beta and IL-17A; the NF-kappaB paradigm. J. Immunol. *183*, 6236–6243.

Gonzalez, R., Jennings, L.L., Knuth, M., Orth, A.P., Klock, H.E., Ou, W., Feuerhelm, J., Hull, M.V., Koesema, E., Wang, Y., et al. (2010). Screening the mammalian extracellular proteome for regulators of embryonic human stem cell pluripotency. Proc. Natl. Acad. Sci. USA *107*, 3552–3557.

Gray, T.E., Guzman, K., Davis, C.W., Abdullah, L.H., and Nettesheim, P. (1996). Mucociliary differentiation of serially passaged normal human tracheobronchial epithelial cells. Am. J. Respir. Cell Mol. Biol. *14*, 104–112.

Gray, T., Coakley, R., Hirsh, A., Thornton, D., Kirkham, S., Koo, J.S., Burch, L., Boucher, R., and Nettesheim, P. (2004). Regulation of MUC5AC mucin secretion and airway surface liquid metabolism by IL-1beta in human bronchial epithelia. Am. J. Physiol. Lung Cell. Mol. Physiol. *286*, L320–L330.

Grünig, G., Warnock, M., Wakil, A.E., Venkayya, R., Brombacher, F., Rennick, D.M., Sheppard, D., Mohrs, M., Donaldson, D.D., Locksley, R.M., and Corry, D.B. (1998). Requirement for IL-13 independently of IL-4 in experimental asthma. Science *282*, 2261–2263.

Guseh, J.S., Bores, S.A., Stanger, B.Z., Zhou, Q., Anderson, W.J., Melton, D.A., and Rajagopal, J. (2009). Notch signaling promotes airway mucous metaplasia and inhibits alveolar development. Development *136*, 1751–1759.

Hogg, J.C., Chu, F., Utokaparch, S., Woods, R., Elliott, W.M., Buzatu, L., Cherniack, R.M., Rogers, R.M., Sciurba, F.C., Coxson, H.O., and Paré, P.D. (2004). The nature of small-airway obstruction in chronic obstructive pulmonary disease. N. Engl. J. Med. *350*, 2645–2653.

Jaffe, A.B., Kaji, N., Durgan, J., and Hall, A. (2008). Cdc42 controls spindle orientation to position the apical surface during epithelial morphogenesis. J. Cell Biol. *183*, 625–633.

Johnson, J.R., Wiley, R.E., Fattouh, R., Swirski, F.K., Gajewska, B.U., Coyle, A.J., Gutierrez-Ramos, J.C., Ellis, R., Inman, M.D., and Jordana, M. (2004). Continuous exposure to house dust mite elicits chronic airway inflammation and structural remodeling. Am. J. Respir. Crit. Care Med. *169*, 378–385.

Kettle, R., Simmons, J., Schindler, F., Jones, P., Dicker, T., Dubois, G., Giddings, J., Van Heeke, G., and Jones, C.E. (2010). Regulation of neuregulin 1beta1-induced MUC5AC and MUC5B expression in human airway epithelium. Am. J. Respir. Cell Mol. Biol. *42*, 472–481.

Kim, Y.D., Kwon, E.J., Park, D.W., Song, S.Y., Yoon, S.K., and Baek, S.H. (2002). Interleukin-1beta induces MUC2 and MUC5AC synthesis through cyclooxygenase-2 in NCI-H292 cells. Mol. Pharmacol. *62*, 1112–1118.

Kudo, M., Melton, A.C., Chen, C., Engler, M.B., Huang, K.E., Ren, X., Wang, Y., Bernstein, X., Li, J.T., Atabai, K., et al. (2012). IL-17A produced by αβ T cells drives airway hyper-responsiveness in mice and enhances mouse and human airway smooth muscle contraction. Nat. Med. *18*, 547–554.

Kuperman, D.A., Huang, X., Koth, L.L., Chang, G.H., Dolganov, G.M., Zhu, Z., Elias, J.A., Sheppard, D., and Erle, D.J. (2002). Direct effects of interleukin-13 on epithelial cells cause airway hyperreactivity and mucus overproduction in asthma. Nat. Med. *8*, 885–889.

Kuyper, L.M., Paré, P.D., Hogg, J.C., Lambert, R.K., Ionescu, D., Woods, R., and Bai, T.R. (2003). Characterization of airway plugging in fatal asthma. Am. J. Med. *115*, 6–11.

Lamar, E., Deblandre, G., Wettstein, D., Gawantka, V., Pollet, N., Niehrs, C., and Kintner, C. (2001). Nrarp is a novel intracellular component of the Notch signaling pathway. Genes Dev. *15*, 1885–1899.

Lange, P., Parner, J., Vestbo, J., Schnohr, P., and Jensen, G. (1998). A 15-year follow-up study of ventilatory function in adults with asthma. N. Engl. J. Med. *339*, 1194–1200.

Laoukili, J., Perret, E., Willems, T., Minty, A., Parthoens, E., Houcine, O., Coste, A., Jorissen, M., Marano, F., Caput, D., and Tournier, F. (2001). IL-13 alters mucociliary differentiation and ciliary beating of human respiratory epithelial cells. J. Clin. Invest. *108*, 1817–1824.

Levine, S.J., Larivée, P., Logun, C., Angus, C.W., Ognibene, F.P., and Shelhamer, J.H. (1995). Tumor necrosis factor-alpha induces mucin hypersecretion and MUC-2 gene expression by human airway epithelial cells. Am. J. Respir. Cell Mol. Biol. *12*, 196–204.

Li, K., Li, Y., Wu, W., Gordon, W.R., Chang, D.W., Lu, M., Scoggin, S., Fu, T., Vien, L., Histen, G., et al. (2008). Modulation of Notch signaling by antibodies specific for the extracellular negative regulatory region of NOTCH3. J. Biol. Chem. *283*, 8046–8054.

Morimoto, M., Liu, Z., Cheng, H.T., Winters, N., Bader, D., and Kopan, R. (2010). Canonical Notch signaling in the developing lung is required for determination of arterial smooth muscle cells and selection of Clara versus ciliated cell fate. J. Cell Sci. *123*, 213–224.

Morimoto, M., Nishinakamura, R., Saga, Y., and Kopan, R. (2012). Different assemblies of Notch receptors coordinate the distribution of the major bronchial Clara, ciliated and neuroendocrine cells. Development *139*, 4365–4373.

Munitz, A., Brandt, E.B., Mingler, M., Finkelman, F.D., and Rothenberg, M.E. (2008). Distinct roles for IL-13 and IL-4 via IL-13 receptor alpha1 and the type II IL-4 receptor in asthma pathogenesis. Proc. Natl. Acad. Sci. USA *105*, 7240–7245.

Rackley, C.R., and Stripp, B.R. (2012). Building and maintaining the epithelium of the lung. J. Clin. Invest. *122*, 2724–2730.

Rock, J.R., Onaitis, M.W., Rawlins, E.L., Lu, Y., Clark, C.P., Xue, Y., Randell, S.H., and Hogan, B.L. (2009). Basal cells as stem cells of the mouse trachea and human airway epithelium. Proc. Natl. Acad. Sci. USA *106*, 12771–12775.

Rock, J.R., Gao, X., Xue, Y., Randell, S.H., Kong, Y.Y., and Hogan, B.L. (2011). Notch-dependent differentiation of adult airway basal stem cells. Cell Stem Cell *8*, 639–648.

Shaykhiev, R., Zuo, W.L., Chao, I., Fukui, T., Witover, B., Brekman, A., and Crystal, R.G. (2013). EGF shifts human airway basal cell fate toward a smoking-associated airway epithelial phenotype. Proc. Natl. Acad. Sci. USA *110*, 12102–12107.

Stahl, M., Uemura, K., Ge, C., Shi, S., Tashima, Y., and Stanley, P. (2008). Roles of Pofut1 and O-fucose in mammalian Notch signaling. J. Biol. Chem. *283*, 13638–13651.

Tsao, P.N., Vasconcelos, M., Izvolsky, K.I., Qian, J., Lu, J., and Cardoso, W.V. (2009). Notch signaling controls the balance of ciliated and secretory cell fates in developing airways. Development *136*, 2297–2307.

Vermeer, P.D., Harson, R., Einwalter, L.A., Moninger, T., and Zabner, J. (2003). Interleukin-9 induces goblet cell hyperplasia during repair of human airway epithelia. Am. J. Respir. Cell Mol. Biol. *28*, 286–295.

Wills-Karp, M. (2004). Interleukin-13 in asthma pathogenesis. Immunol. Rev. *202*, 175–190.

Wills-Karp, M., Luyimbazi, J., Xu, X., Schofield, B., Neben, T.Y., Karp, C.L., and Donaldson, D.D. (1998). Interleukin-13: central mediator of allergic asthma. Science *282*, 2258–2261.

Woodruff, P.G., Modrek, B., Choy, D.F., Jia, G., Abbas, A.R., Ellwanger, A., Koth, L.L., Arron, J.R., and Fahy, J.V. (2009). T-helper type 2-driven inflammation defines major subphenotypes of asthma. Am. J. Respir. Crit. Care Med. *180*, 388–395.

Wu, Y., Cain-Hom, C., Choy, L., Hagenbeek, T.J., de Leon, G.P., Chen, Y., Finkle, D., Venook, R., Wu, X., Ridgway, J., et al. (2010). Therapeutic antibody targeting of individual Notch receptors. Nature *464*, 1052–1057.

Wu, X., Peters-Hall, J.R., Bose, S., Peña, M.T., and Rose, M.C. (2011). Human bronchial epithelial cells differentiate to 3D glandular acini on basement membrane matrix. Am. J. Respir. Cell Mol. Biol. *44*, 914–921.